Role of Constraints in Inverse Design for Transonic Airfoils

G. Volpe* and R.E. Melnik†
Grumman Aerospace Corporation, Bethpage, New York

This paper deals with the problem of determining an airfoil shape that corresponds to a prescribed pressure distribution. Lighthill's exact solution of this problem in incompressible flow demonstrated that the surface pressure distribution and the freestream speed cannot both be prescribed independently. This implies the existence of a constraint on the prescribed pressure distribution. The same constraint exists at compressible speeds. The present paper describes a new method for solving the inverse problem at transonic speeds, one that does not violate this constraint. In the method, the target pressure distribution contains a free parameter that is adjusted during the computation to assure the existence of a solution to the inverse problem. The computational scheme is based on the numerical solution of the full potential equation. Several examples are presented.

Introduction

THE design goal of improved aircraft aerodynamic efficiency often leads to the tailoring of the airfoil to specific commercial or military requirements. The aircraft design may call for the wing profile to have certain lift and/or drag characteristics, a particular lift distribution, or a specific velocity distribution that would provide a measure of control on boundary-layer behavior. In such cases, the airfoil design problem is reduced to the specification of a desired pressure distribution—or, equivalently, speed distribution. This approach leads to the theoretical problem of finding an airfoil shape that produces a desired pressure distribution as closely as possible.

The "inverse" problem of airfoil theory has been of interest for some time and techniques for the construction of practical profiles have been formulated for incompressible flow,[1-6] for subcritical compressible flow,[7] and for supercritical flows.[8,9] For incompressible flow, it was demonstrated by Lighthill[1] that a solution to the inverse problem generally does not exist unless the prescribed speed distribution satisfies a certain integral constraint arising from the requirement that the speed in the freestream be equal to one (or any other specified value). The additional requirements that the airfoil close (or have a specified trailing-edge thickness) and be at a given incidence were shown by Lighthill to lead to two additional constraints on the prescribed pressure distribution. Since Lighthill's definitive 1945 paper, it has been clearly recognized that three constraints must be imposed on the prescribed pressure distribution in formulating the inverse design problem. Woods[2] later demonstrated that similar constraints were also required in the mixed-design problem in which the pressure distribution is prescribed for some parts of the airfoil and the shape is prescribed for other parts. For incompressible flow, Lighthill's[1] and Woods'[2] theories led to explicit integral expressions for the constraints. Later, using a Kármán-Tsien model gas approximation, Woods[2] was able to derive similar expressions for the integral constraints for compressible, subcritical flows. These expressions reduce to Lighthill's expressions in the limit of incompressible flow. For a perfect gas in compressible flow, closed-form expressions for closure cannot be derived, but their existence can be inferred from the fact that the incompressible flow case is a subcase of the more general compressible flow problem.

Thus, in order to assure that a solution to the inverse problem exists, some freedom must be permitted in the prescribed pressure distribution to allow the three constraints to be satisfied. This can be accomplished by introducing three free parameters into the prescribed form of the pressure distribution. One parameter is adjusted to satisfy the first constraint arising from the condition that the speed at infinity be one and the other two are adjusted to satisfy the two closure conditions. Alternatively, the angle of attack of the airfoil can be left free (to be determined as part of the solution) and one of the trailing-edge closure conditions and the associated parameter in the pressure distribution can be eliminated. Theoretical studies indicate that, even if conditions on trailing-edge closure are not imposed, one constraint must still be imposed on the prescribed pressures. This situation regarding the proper formulation of the inverse design problem is quite clear for incompressible and compressible subcritical flows. Numerous examples illustrating this point have been presented in the literature.[1-7]

Recently, there have been a number of attempts to develop solution procedures for the inverse problem in compressible, supercritical flow. Unfortunately, none have adequately addressed the role of constraints and the question of the proper formulation of the inverse design problem. Since Woods'[7] analysis is based on the Kármán-Tsien model gas approximation, it is useful only for subcritical flow and has contributed little to our understanding of supercritical problems. Recent attempts by Tranen[8] and Carlson[9] to solve the compressible inverse problem have not satisfactorily addressed the issue of constraints. In their works, Tranen and Carlson have addressed only the question of trailing-edge closure and have completely ignored the question of the first constraint. Tranen enforced trailing-edge closure of the airfoil shape determined from a solution of an inverse problem that was not entirely consistent with the corresponding direct problem and attempted to converge on a pressure distribution "close" to the one sought by iterating through a sequence of inverse and direct problems. Carlson's closure procedure is based on an adjustment of the nose radius to close the trailing edge using a mixed direct-inverse procedure.

Although both procedures seem to be workable approaches to the trailing-edge closure problem, neither method provides a satisfactory solution to the inverse problem, because each lacks consideration of the first constraint and is therefore ill-posed. It is recognized that both methods can reproduce known airfoil sections using pressure distributions taken from

Presented as Paper 81-1233 at the AIAA 14th Fluid and Plasma Dynamics Conference, Palo Alto, Calif., June 23-25, 1981; received Sept. 2, 1983; revision received Feb. 12, 1984.

*Staff Scientist. Member AIAA.
†Director for Fluid Mechanics, Research & Development Center. Member AIAA.

direct solutions. Since such pressure distributions automatically satisfy the constraints, these examples do not provide a real test of the correctness of their formulations of the inverse problem. It is also plausible that these methods can be operated successfully to improve given airfoils by slightly modifying pressure distributions taken from direct solutions. In general, however, they must fail when more general pressure distributions are prescribed.

Similar objections also apply to Henne's[10] recent extension of Tranen's method to three-dimensional wings. For compressible flow, the absence of explicit constraints on the pressure causes no real problems in working out an acceptable formulation to the trailing-edge closure problem. The main impediment to the establishment of a satisfactory formulation of the inverse problem in compressible flow has been the lack of an explicit statement of the first constraint. We know from Lighthill's theory that we must either leave the speed at infinity free or introduce a single degree of freedom into the surface pressure distribution (in addition to the two parameters required for trailing-edge closure) to allow the first constraint to be satisfied. However, in compressible flow, we do not have an explicit condition, analogous to Lighthill's first constraint, that can be used to fix the parameter that must be introduced into the data.

In the present work, we describe a new formulation of the inverse design problem that is aimed at providing a treatment of the constraints on the imposed pressure distribution which is consistent with Lighthill's analysis of the incompressible problem. This paper is concerned only with the first constraint since this has proved to be the most difficult to understand and implement in compressible flows. However, the formulation is easily generalized to deal with the question of trailing-edge closure and the other two constraints by introducing two additional free parameters into the prescribed pressure distribution.

The formulation is consistent with Lighthill's in the sense that a free parameter must be introduced into the boundary data to assure the existence of a solution. Although our solubility condition is analogous to Lighthill's first constraint, we have not yet been able to show that it is precisely equivalent to Lighthill's first integral constraint in incompressible flow. However, the present method does provide a useful approach to the inverse problem at transonic speeds. We have been able to demonstrate through many numerical examples that our method correctly determines the airfoil shape and pressure distribution corresponding to known direct solutions starting from a prescribed pressure differing greatly from the direct solution. In these cases, our solubility condition automatically adjusts a free parameter appearing in the initial prescribed pressure distribution to the correct value corresponding to the known direct solution. Further, if the solubility condition is not imposed and the parameter appearing in the surface pressure distribution is not adjusted, the numerical procedure fails, indicating that a solution of the inverse problem does not exist for the prescribed initial pressure distribution. Examples of airfoils designed with this formulation are presented for both subcritical and supercritical flows with shock waves.

There are, of course, other approaches to the problem of airfoil design at transonic speed based on iterated solutions of the direct problem. In these methods, direct solutions are sought with an airfoil shape modified iteratively to minimize the difference between the computed pressures and a prescribed target pressure distribution. The issue of constraints is avoided in this approach because one is not seeking a closed airfoil for a fixed prescribed pressure distribution, but an airfoil with a pressure distribution or force characteristics "close" to prescribed targets. Recent examples of this type of approach appear in the works of Hicks et al.,[11] Davis,[12] and McFadden.[13] The relative merits of this approach to airfoil design compared to the constrained inverse method described in this paper remain to be established.

Formulation of the Inverse Problem

Using conformal mapping techniques, Lighthill was able to obtain an exact solution for incompressible flow. As part of this solution, it was shown that a solution for a closed airfoil exists only if the prescribed speed satisfies the following three integral constraints:

$$\int_0^{2\pi} \log\left|\frac{q_0}{q_\infty}\right| d\omega = 0 \tag{1}$$

$$\int_0^{2\pi} \log\left|\frac{q_0}{q_\infty}\right| \begin{Bmatrix}\cos\omega\\ \sin\omega\end{Bmatrix} d\omega = 0 \tag{2}$$

where q_0 is the prescribed speed distribution on the airfoil surface, q_∞ the speed at infinity, and ω the polar angle in the transformed plane obtained from the conformal mapping of the airfoil to a circle. The first condition arises from the requirement that the speed at infinity is q_∞, and the other two from the requirement that the airfoil is a closed contour. Lighthill demonstrated that, if Eqs. (1) and (2) are satisfied, the desired airfoil shape can be determined from q_0 by simple quadratures. Lighthill presented examples in which the speed distribution was prescribed in the terms of the circle plane angle ω and three free constants in the form

$$q_0/q_\infty = f_\omega(\omega; A, B, C) \tag{3}$$

where the three parameters were chosen to satisfy the integral constraints. This provides only an indirect solution to the design problem in that the speed distribution in the physical plane $q_0(s)$ is not known in advance but can only be determined, after the fact, from the conformal transformation specifying ω as a function of s (where s is the arc length on the airfoil surface). Arlinger,[4] Strand,[5] and Polito[6] showed how Lighthill's solution can be embedded in an iterative scheme in which the speed distribution is prescribed in the physical plane as a function of arc length in the form,

$$q_0/q_\infty = f_s(s; A, B, C) \tag{4}$$

Our approach to the inverse problem recognizes the need to account for constraints on the prescribed speed distribution. Here, we ignore the trailing-edge closure conditions in order to focus on the more difficult question of the first constraint. In this case, the prescribed surface speed must contain just one free parameter and we accept airfoil solutions independent of the magnitude of the trailing-edge gap. Thus, we assume the surface speed distribution is prescribed in the form,

$$q_0/q_\infty = f(s; A) \tag{5}$$

where A is a free parameter. Of course, the particular form chosen will affect the class of airfoil solutions that can be obtained. In the present work, we assume the particular form

$$q_0/q_\infty = Af(s) \tag{6}$$

where the amplitude A is a parameter that is determined as part of the solution and $f(s)$ a given function that specifies the shape of the surface speed distribution. It is possible to proceed in two ways: either A is left free and the freestream speed q_∞ is set to one or, alternatively, the surface speed distribution is completely fixed but the freestream is left free to be determined as part of the solution. Since both procedures are entirely equivalent, we can, without loss of generality, choose the latter approach by defining $A = 1/q_\infty$ with q_∞ taken as an arbitrary parameter, identified with the value of q in the freestream.

If the freestream Mach number were zero, we could determine the value of q_∞ from the first constraint in Lighthill's

solution. In this case, with $A = 1/q_\infty$, substitution of Eq. (5) into Eq. (1) yields,

$$q_\infty(M_\infty = 0) = \exp\left[\frac{1}{2\pi}\int_0^{2\pi} \log|f(s)|\,d\omega\right] \tag{7}$$

An explicit condition to determine q_∞, comparable to Eq. (7), is not known for compressible flow. Fortunately, a solubility condition arises at a given point in our formulation that fills the role of Eq. (7) in providing a condition for determining the value of q_∞. In our approach, we specify the shape function $f(s)$, make an initial estimate of the value of q_∞, and then integrate the speed distribution specified by Eq. (6) to determine the values of surface velocity potential. Using an estimate for the airfoil shape, we then conformally map the approximate airfoil to a unit circle ($r = 1$). Using the resulting surface potential and approximate mapping modulus, we then solve the resulting Dirichlet problem for the full potential equation using a mixed relaxation technique in the (approximate) circle plane. If the computed velocity component normal to the circle representing the transformed airfoil shape turns out to be zero at every point on the surface, the approximate airfoil is a streamline and the inverse solution is completed. In general, the normal velocity is nonzero on the boundary. In this case, the values of the normal velocity provide the information necessary to correct the estimate for the airfoil geometry as follows. If v and u are the velocity components along the r, ω coordinate directions in the circle plane, the flow angle perturbation at the airfoil surface is given by

$$\delta\theta = \tan^{-1}\left[\frac{v(r=1,\omega)}{u(r=1,\omega)}\right] \tag{8}$$

The quantity $\delta\theta(\omega)$ is the local angle through which the approximate airfoil surface must be rotated to make it a streamline. We employ the perturbation slope $\delta\theta(\omega)$ in the conjugate relations connecting the mapping modulus and the airfoil slope defining the conformal mapping of the airfoil to the unit circle. These relations then determine the corrections to the mapping modulus that will drive the approximate airfoil surface to become a streamline. At convergence, the normal velocity component at the surface ($r = 1$) is zero at every point, giving a zero flow angle correction and a converged mapping modulus. At this point, the inverse mapping of the unit circle to the converged airfoil shape can be carried out by Fourier series using the now known mapping modulus and airfoil slope distribution.

At a given stage of the iteration, the computed normal velocity component v generally does not vanish at the points where the prescribed surface speed u has a zero. Consequently, the procedure described above will fail because the flow angle corrections $\delta\theta$ at these points are unbounded. In order to assure that a solution exists, we must therefore impose the conditions that the normal velocity component v vanishes at the points where the prescribed surface speed is zero. If ω^* denotes the value of ω where u (or q_0) is zero, the resulting condition can be written as

$$v(r=1, \omega=\omega^*) = 0 \tag{9}$$

This condition is equivalent to requiring those points where the surface speed vanishes to be stagnation points and to remain so at each step of the solution. Physically, this is related to the requirement that a curve on which the speed distribution is prescribed be a stream surface. This condition apparently can be satisfied only if the zeroes of q_0 [or $f(s)$] are stagnation points that permit a branching of the streamlines. In the present work, we present examples only of cusped airfoils for which there is only one stagnation point—generally, on the forward part of the airfoil. In this case, Eq. (9) serves as the single condition determining the value of q_∞. If an airfoil has a wedge-shaped trailing edge, an additional stagnation point arises at the trailing edge. Although we will not consider this more general class of airfoil profiles here, we should note that the present method does apply and can be used to design such airfoils.

We have not been able to analytically demonstrate that our solubility condition in Eq. (9) is equivalent to Lighthill's first constraint and reduces to it [Eq. (1)] in the incompressible limit ($M_\infty = 0$). Nevertheless, numerical experiments reported in this paper suggest that this is the case and that Eq. (9) correctly determines the airfoil shape when the shape function $f(s)$ is taken from a direct solution, independent of the starting value taken for the amplitude parameter, $A = 1/q_\infty$. Moreover, the present results clearly indicate that the selection of the shape of the prescribed speed distribution $f(s)$ is by itself sufficient to determine the airfoil shape. The additional specification of the amplitude parameter A would clearly overspecify the data and lead to an ill-posed problem. Although not conclusive, results obtained to date indicate that the solutions are unique in the sense that there appears to be only one airfoil shape and one value of the amplitude parameter corresponding to each choice of the shape function $f(s)$. Further details on the numerical implementation of the method are given in the following section.

Inverse Method of Design

The problem addressed in this section is that of finding an airfoil shape having a velocity distribution prescribed to be

$$\frac{q_0}{q_\infty} = \frac{1}{q_\infty} f\left(\frac{s}{s_{\max}}\right) \tag{10}$$

where q_∞ is a constant to be determined as part of the solution. The point $s = 0$ corresponds to the lower surface trailing-edge point and $s = s_{\max}$ is the corresponding point on the upper surface. One is free to pick the angle of attack α of the freestream. Different choices of α will result in different orientations of the designed airfoil with respect to the far field, the contour being otherwise identical. The design procedure requires that a starting airfoil shape be prescribed to provide an initial boundary. With $q_0 = f(s)$ prescribed as the tangential velocity on this contour, the resulting Dirichlet problem for the flowfield around the contour can be solved and the difference between the original contour and a streamline can be estimated. The actual solution process is carried out by mapping the approximate airfoil contour to a unit circle. The approximate airfoil shape is then modified and the process repeated until the airfoil boundary is reduced to be a streamline of the flow.

Mapping Procedures

Our procedure is based on the conformal mapping of the approximate airfoil shape to unit circle using the slope-type mapping procedure described by Van Ingen[3] and employed in Jameson's[14] relaxation methods. The derivative of the mapping function $z(\zeta)$ is represented as a finite power series in the form

$$\frac{dz}{d\zeta} = \left(1 - \frac{1}{\zeta}\right)^{(1-\epsilon)} e^{P+iQ} \tag{11}$$

where

$$P = \sum_{n=0}^{N} (A_n \cos n\omega + B_n \sin n\omega) \tag{12}$$

$$Q = \sum_{n=0}^{N} (A_n \sin n\omega - B_n \cos n\omega) \tag{13}$$

In these expressions ($\epsilon\pi$) is the included angle at the trailing edge, $z = x + iy$ is the complex coordinate in the original

airfoil plane, $\zeta = re^{i\omega}$ is the complex coordinate (with r and ω the polar coordinates) in the circle plane, and A_n, B_n are the constants defining the mapping. Separation of Eq. (11) into its real and imaginary parts leads to

$$\frac{ds}{d\omega} = \left[2\sin\left(\frac{\omega}{2}\right)\right]^{(1-\epsilon)} e^{P} \tag{14}$$

$$\theta = \tfrac{1}{2}(1+\epsilon)(\pi-\omega) - (\pi/2) + Q \tag{15}$$

where θ is equal to the local slope of the airfoil.

As discussed in Jameson,[14] this mapping procedure has the advantage that it permits a profile with an open tail to be mapped to a closed circle.

In practice, the mapping of the airfoil is implemented from a knowledge of the values of the airfoil slope at $2N$ points distributed around the unit circle. From these known values, the coefficients A_n, B_n are determined from a Fourier analysis of $\theta(\omega)$ using Eq. (15).

Solution of Flowfield in the Circle Plane

We base our solution on the full potential equation in a nonconservative form. We employ a nonconservative version of Jameson's[14] mixed-flow relaxation method modified to accept Dirichlet-type boundary conditions. In the absence of boundary-layer effects in the formulation, this type of numerical scheme yields solutions that agree better with experimental data than the solutions obtained by conservative schemes. The use of such a scheme is only a matter of choice and not essential to the design procedure. A fully conservative design method can be set up in a similar manner.

The potential equation for irrotational flow in polar coordinates is

$$(a^2-u^2)G_{\omega\omega} - 2uv(rG_{\omega r} + G_\omega - E) + (a^2-v^2)(r^2G_{rr} + rG_r) + (u^2-v^2)rG_r + (u^2+v^2)\left(\frac{u}{r}h_\omega + vh_r\right) = 0 \tag{16}$$

where a is the local speed of sound and the velocity components in the two coordinates directions u, v are given in terms of a reduced velocity potential G by

$$u = \frac{r}{h}\left[G_\omega - E - \frac{q_\infty}{r}\sin(\omega+\alpha)\right] \tag{17}$$

$$v = \frac{r}{h}\left[rG_r - \frac{q_\infty}{r}\cos(\omega+\alpha)\right] \tag{18}$$

where α is the angle of attack, E the circulation constant, and h the modulus of the conformal transformation of the region exterior to the airfoil surface to the interior of the unit circle and is given in terms of the mapping function by

$$h = \frac{1}{r^2}\left|\frac{dz}{d\zeta}\right| \tag{19}$$

Here G is a reduced potential obtained by subtracting the freestream and circulatory parts of the flow from the full potential ϕ,

$$G = \phi - \frac{q_\infty}{r}\cos(\omega+\alpha) + E(\omega+\alpha) \tag{20}$$

In the far field ($r = 0$), G has the behavior indicated by Ludford[15]

$$G = G_\infty + E\left\{(\omega+\alpha) - \tan^{-1}\left[\sqrt{1-M_\infty^2}\tan(\omega+\alpha)\right]\right\} \tag{21}$$

where G_∞ is an arbitrary constant that can be set to zero in direct problems, but which must be determined as part of the solution in inverse problems by extrapolation from the interior of the flowfield.

For the direct problem, we set $q_\infty = 1$ and the solution to Eq. (16) is then obtained by standard relaxation procedures using a uniform polar coordinate grid in the circle plane. The surface boundary condition is satisfied by setting the value of the potential on a "dummy" point beyond the surface to make $v = 0$ the surface ($r = 1$). The introduction of the "dummy" points is a numerical device to satisfy the boundary conditions, without having to write special difference formulas on the boundary. The circulation constant E is evaluated by requiring $u = 0$ at the trailing edge in Eq. (17).

To find the solution of the inverse problem, it is first necessary to set up the boundary conditions at the contour surface. The assumed initial contour provides initial estimates for the mapping modulus h and the arc-length relation, $s = s(\omega)$, which makes it possible to set up the desired velocity q_0 as a function of the circle angle ω through interpolation from the original $q_0 = f(s)$. In the circle plane, q_0 is identified with the tangential velocity u. Of course, this will be true only when the solution process is fully converged. Having obtained u at midpoints of the grid, the circulation can be computed as

$$E = \frac{1}{2\pi}\sum_{n=1}^{M}(hu)_{n+\frac{1}{2}}\Delta\omega \tag{22}$$

where $\Delta\omega$ is the grid width and M the number of grid points in the circumferential direction. Assuming a value G_0 for the potential at the lower surface trailing edge, the potential around the contour is obtained by integration from (hu). Thus

$$G_n = G_0 + \sum_{n=1}^{M}\left[(hu)_{n+\frac{1}{2}} + E + q_\infty\sin(\omega+\alpha)\right]\Delta\omega \tag{23}$$

where G_0 is a constant that may be arbitrarily prescribed without loss of generality (since we have left a corresponding constant G_∞ appearing in the far-field behavior free to be determined as part of the solution).

The initial value of q_∞ is also arbitrary and is usually chosen to be one. Since there is no control on the value of the normal velocity at the airfoil surface, there will, in general, be a net mass flow emitted from the boundary. To allow for this, we subtract a source term $[\sigma\log r]$ from the reduced potential leading to the following definition of G:

$$G = \bar{G} + \sigma\log r \tag{24}$$

An additional source term $\{\sigma/2\log[1 - M_\infty^2\sin^2(\omega+\alpha)]\}$ also appears in the far-field boundary condition.

In this Dirichlet problem, this source term has a role similar to that of the circulation term in the Neumann problem. The value of α is obtained by setting v equal to zero at the trailing edge. The introduction of the source term guarantees compatibility of surface and far-field boundary conditions. As the design process converges, the value of σ goes to zero for low-speed flow. For flows with shock waves, it settles down to values reflecting the mass generation at shock waves introduced by the nonconservative differencing.

With the boundary conditions established at the surface, the flowfield within the circle can be solved as in the direct case. The potential at the "dummy" point beyond the surface is given the value that satisfies the difference equation at the boundary point ($r = 1$). The normal velocity at the surface can then be calculated at the boundary using the dummy value of the potential. At the end of each sweep, q_∞ and σ are found by setting the normal velocity component to zero, giving

$$\bar{G}_\omega + \sigma - q_\infty\cos(\omega-\alpha) = 0 \tag{25}$$

at both the leading-edge stagnation point and the trailing edge. The reduced potential at the boundary is readjusted to

reflect the new value of q_∞ in order that the tangential velocity on the surface remain the same.

Contour Modification

A nonzero normal velocity v at the boundary implies that the actual streamline is (to first order) rotated from the boundary by an angle equal to

$$\delta\theta = \tan^{-1}(v/u) \tag{26}$$

Denoting the new values of a variable by $\tilde{(\ )}$ and changes in that variable by $\delta(\ )$, the new contour is mapped to a circle by a transformation similar to Eq. (11)

$$\frac{dz}{d\zeta} = \left(1 - \frac{1}{\zeta}\right)^{(1-\tilde{\epsilon})} e^{\tilde{P}+i\tilde{Q}} \tag{27}$$

which implies relations similar to Eqs. (12) and (13). If one lets

$$\tilde{P} = P + \delta P = \sum_{n=1}^{M/2} \left(\tilde{A}_n \cos n\omega + \tilde{B}_n \sin n\omega\right) \tag{28}$$

then

$$\delta\theta - \frac{1}{2}\delta\epsilon(\pi - \omega) = \delta Q = \sum_{n=1}^{M/2} \left(A'_n \sin n\omega - B'_n \cos n\omega\right) \tag{29}$$

where

$$\delta\epsilon = (1/\pi)(\delta\theta_1 - \delta\theta_M),$$

$$A'_n = \tilde{A}_n - A_n, \quad \text{and} \quad B'_n = \tilde{B}_n - B_n \tag{30}$$

From the solution to the Dirichlet problem and Eq. (26), $\delta\theta$ is known as a function of ω. By a standard Fourier analysis of Eq. (29), A'_n and B'_n are then evaluated. Values of the updated Fourier coefficients of the full series for the transformation, $\tilde{A}_n$ and $\tilde{B}_n$, can then be formed. The arc length derivative $ds/d\omega$ can be calculated from Eqs. (14) and (15) and then,

$$\frac{d\tilde{x}}{d\omega} = -\frac{d\tilde{s}}{d\omega}\cos\tilde{\theta}, \qquad \frac{d\tilde{y}}{d\omega} = -\frac{d\tilde{s}}{d\omega}\sin\tilde{\theta} \tag{31}$$

Integration then yields $\tilde{s}(\omega)$, $\tilde{x}(\omega)$, and $\tilde{y}(\omega)$.

The solution of the flowfield was obtained using the metric from an initially assumed shape and the boundary conditions were based on the corresponding $s(\omega)$. The Dirichlet problem is then solved again with the new values for these quantities. There is, however, no need at any stage to do a direct solution over the current airfoil contour. Such a calculation is desirable at convergence in order to check the accuracy of inverse solution. The iteration process is continued until a desired tolerance in the maximum value of $|v/u|$ is reached. At this point, the tangential velocity u will be equal to the total speed prescribed at the airfoil surface. Also the value of q_∞ will have been found.

To ensure convergence of the design process, it was necessary to under-relax the changes to the contour shape. Thus, only a fraction, typically 25%, of the change in slope suggested by Eq. (26) is actually taken in the early design cycles. After several contour modifications, the factor can be increased. The tangential velocity $u(\omega)$ at the boundary, which is interpolated from the desired $q_0 = f(s)$, is also under-relaxed when starting a new design cycle.

Results

The obvious, most basic, test case of an inverse design method is the reproduction of an airfoil, using as input the pressure distribution generated by a direct solution of the flow over the airfoil. In all the cases presented, the angle of attack in the inverse problem is chosen to be zero and the freestream speed is computed as part of the solution. All results for pressure are given in terms of a pressure coefficient defined in terms of the computed freestream speed.

The first example is that of a Korn airfoil at $M_\infty = 0.1$ and $\alpha = 1.7$ deg. In this case, we seek to compute the original Korn airfoil shape from a prescribed pressure distribution that is taken from a direct relaxation solution. The direct solution for the pressure distribution is depicted in Fig. 1. The starting profile for the inverse design procedure was chosen to be the NACA 0010 airfoil. The Korn airfoil shape is essentially recovered after 18 design cycles. The largest error in the coordinates at this stage of the design is less than 0.1%. The designed airfoil is rotated in a clockwise direction by 1.7 deg with respect to the original airfoil. This is a result of setting the angle of attack to zero in the inverse method. If it had been chosen to be 1.7 deg, the designed airfoil would have the same orientation as the original profile (this has been checked). In the present case, the target pressure distribution is obtained when the designed shape is analyzed in a direct mode at an angle of attack of zero as seen in Fig. 2. Figure 3 gives the rates of convergence for the maximum value of $|v/u|$ and for the mass flow parameter σ. This being an essentially incompressible case, σ goes to zero as expected. The initial choice of the freestream speed was set to one (as we do in most cases) and remained at this value to better than three decimal places. The "wiggle" between iterations 5 and 6 is due to an abrupt increase of the relaxation factors employed in this calculation.

A more meaningful test is to repeat the calculation with the same prescribed surface speed but with a different choice for the initial guess of the freestream speed. Since the prescribed speed distribution was obtained from a direct solution with $q_\infty = 1$, the computed value of q_∞ in the inverse calculation should approach one, independent of its chosen initial value. Results given in Fig. 4 clearly demonstrate that the computed

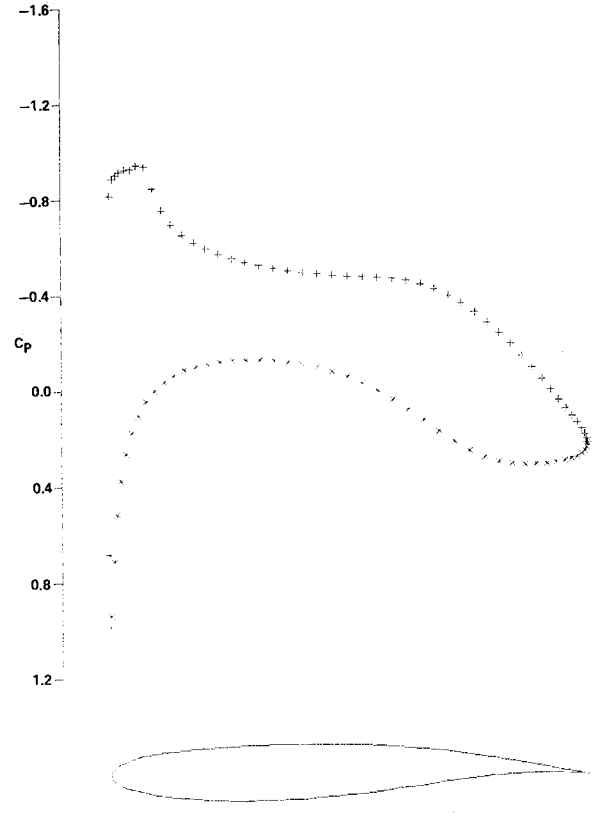

Fig. 1 Pressure distribution on Korn airfoil ($M_\infty = 0.100$, $\alpha = 1.7$ deg, $C_L = 0.5262$, $C_D = -0.0001$).

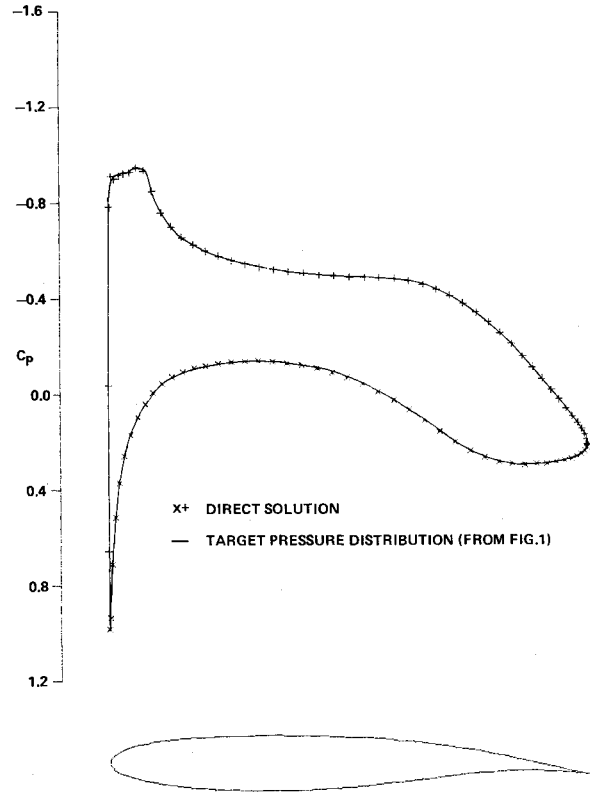

Fig. 2 Designed airfoil contour and direct solution ($M_\infty = 0.100$, $\alpha = 0$ deg, $C_L = 0.5266$, $C_D = -0.0001$).

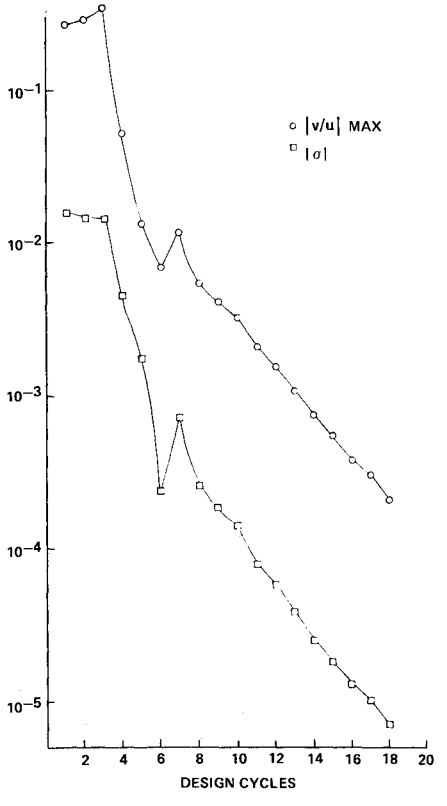

Fig. 3 Convergence history maximum surface velocity ratio and mass flow coefficient for Korn airfoil design ($M_\infty = 0.100$).

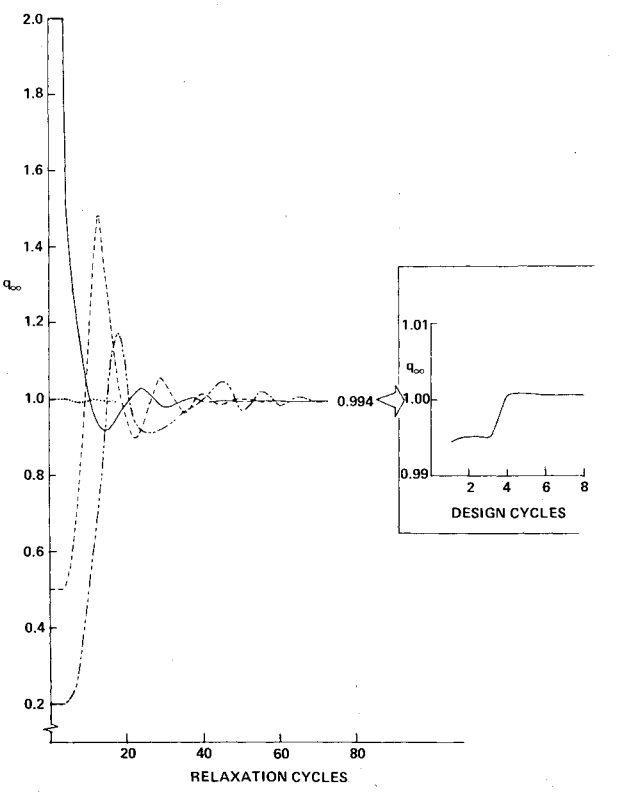

Fig. 4 Convergence history of scale factor for Korn airfoil design ($M_\infty = 0.100$).

freestream speed approaches one, to within the truncation error of the scheme, for arbitrarily selected values of q_∞ chosen in the range $0.2 \le q_\infty \le 2$. These results provide strong evidence to our assertion that the freestream speed cannot be set independently of the prescribed surface speed distribution, but is in fact determined as part of the inverse solution. These results can also be interpreted as a calculation carried out by multiplying the surface speed distribution by an arbitrary amplitude factor and keeping the freestream speed fixed at one. The results in Fig. 4 can then be interpreted as the convergence of the amplitude factor to one as the iteration proceeds. Interpreted in this way, our results indicate that the airfoil shape is completely determined by the shape of the surface speed distribution and not by its amplitude. Existing inverse codes of the Tranen and Carlson type would likely fail if they were employed to find airfoil shapes corresponding to pressure distributions generated in this manner.

The advantage of the present formulation over the use of Eq. (1) is that it can be used at supercritical speeds. Thus, if the pressure distribution generated by an analysis of the Korn airfoil at $M_\infty = 0.75$, $\alpha = 1.7$ deg is specified as a target, the airfoil is once again recovered exactly, as seen in Fig. 5. The starting contour was again the NACA 0010 profile. Figures 6 and 7 give the slope distributions in the leading-edge region of the airfoil and in the region near the shock wave position. The addition of 1.7 deg to the slope of the designed airfoil is due to the rotation of the airfoil mentioned above. It is seen that even in the latter case the shape is recovered without any "wiggles" near the shock wave. The points defining the designed shape are those corresponding to the grid points of the computational mesh.

The present method does not control the extent of the trailing-edge gap, but accepts whatever trailing-edge configuration results from the computation. The Korn airfoil is a closed profile and the cases presented correctly predicted a closed trailing edge. In the case shown in Fig. 8, the gap is not zero. The target pressure distribution depicted by the solid

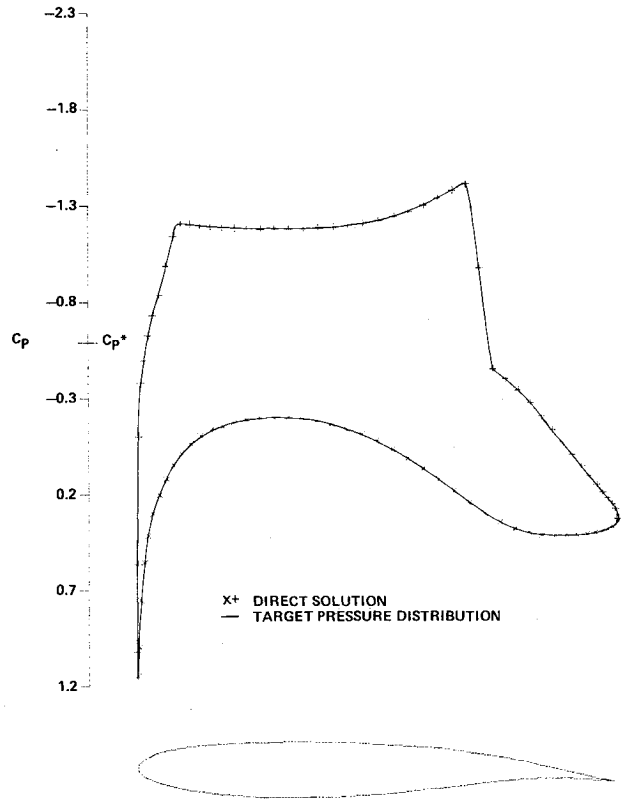

Fig. 5 Designed airfoil contour and direct solution ($M_\infty = 0.750$, $\alpha = 0$ deg, $C_L = 0.9769$, $C_D = 0.0277$).

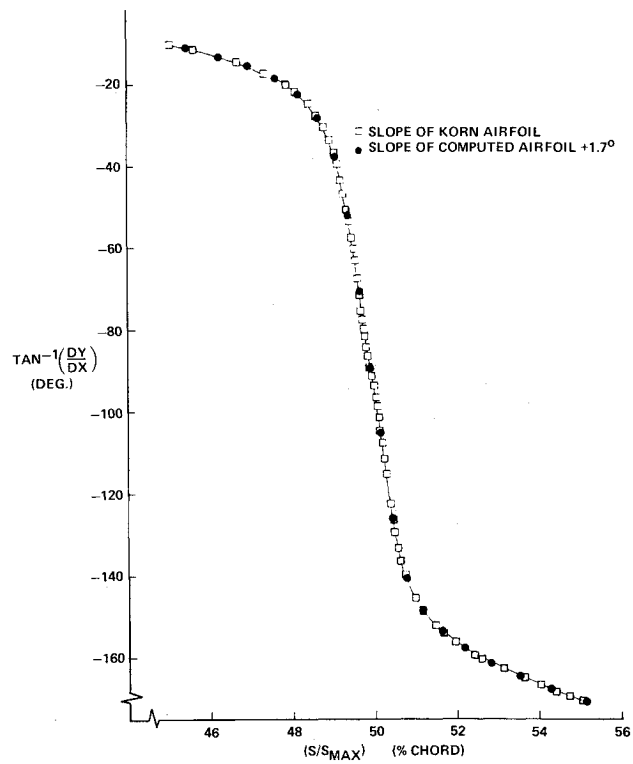

Fig. 6 Computed and actual slope distribution for Korn airfoil design in the leading edge region [$M_\infty = 0.750$, $\alpha = 1.7$ deg (actual contour), $\alpha = 0$ deg (designed contour)].

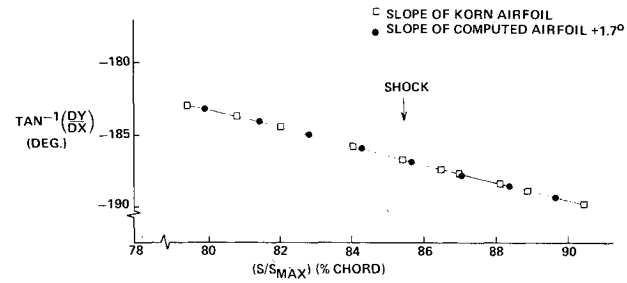

Fig. 7 Computed and actual slope distribution for Korn airfoil design in shock wave region [$M_\infty = 0.750$, $\alpha = 1.7$ deg (actual contour), $\alpha = 0$ deg (designed contour)].

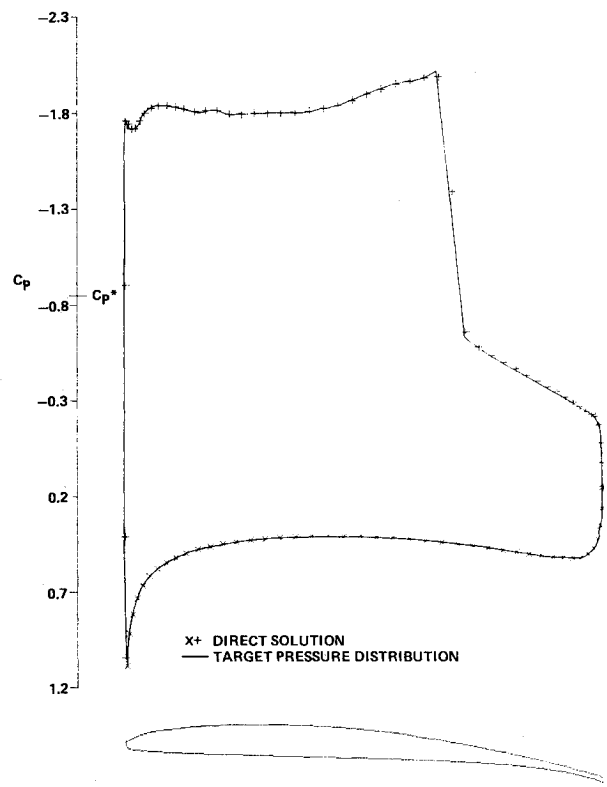

Fig. 8 Designed airfoil contour and direct solution ($M_\infty = 0.683$, $\alpha = 0$ deg).

line in Fig. 8 is generated, again, by a direct solution. It is obtained and the profile recovered starting from the Korn profile, exactly as seen in Fig. 8. Again, the correct trailing-edge gap is predicted.

Figures 9 and 10 are examples of a series of airfoils designed by the method at a Mach number of 0.8. In each case the target upper surface distribution was the same. The prescription varies on the lower surface and in the leading-edge region. The computed values for freestream velocity are indicated in the figure captions of each of these results and are different in each case. Because of the changes in the computed freestream speed, the pressure coefficient distributions on the upper surfaces were also changed in the converged results by factors depending on the magnitude of the computed freestream speed.

The last example in Fig. 11 is the result of changing the prescription for the pressure distribution on the lower surface and in the leading-edge region to obtain $q_\infty \approx 1$ and a zero trailing-edge thickness. The results in Fig. 11 indicate that these goals were achieved. However, a crossover of the upper

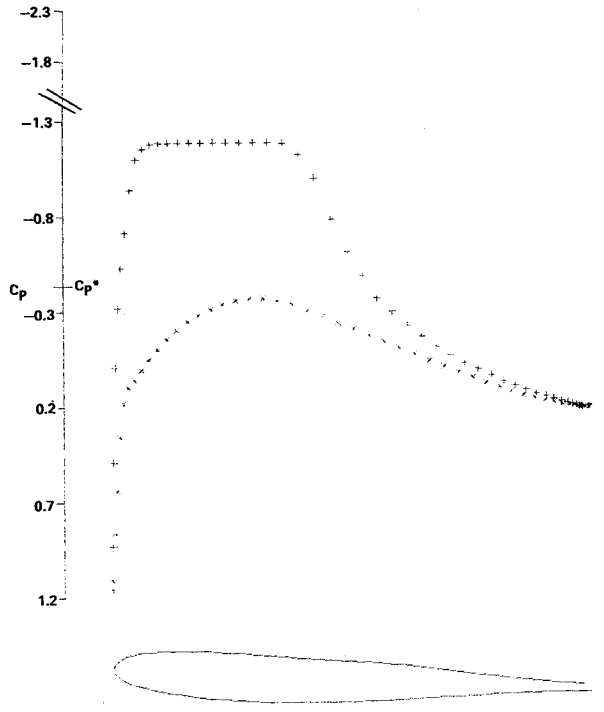

Fig. 9 Design case 845: contour and direct solution [$M_\infty = 0.800$, $C_L = 0.4678$ ($q_\infty = 1.006$)].

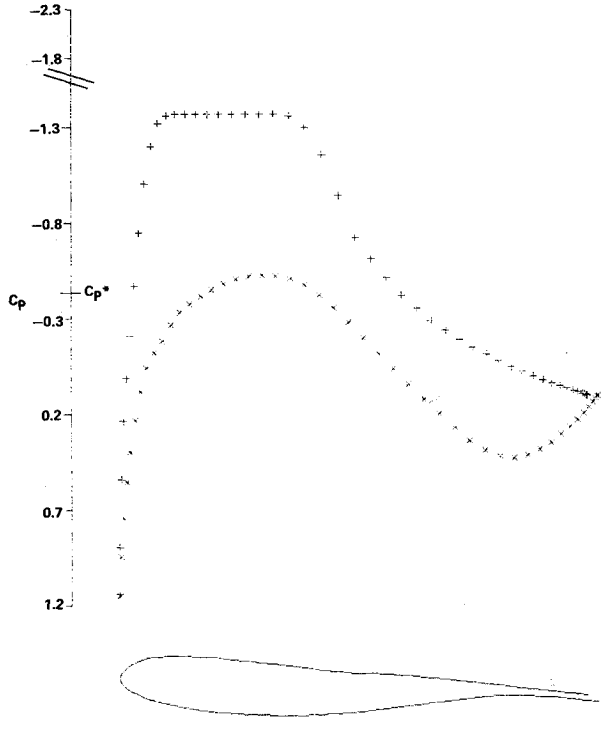

Fig. 10 Design case 731: contour and direct solution [$M_\infty = 0.800$, $C_L = 0.6221$ ($q_\infty = 0.945$)].

and lower surfaces occurs at about 90% chord, resulting in a negative thickness and an unacceptable airfoil profile.

Except for the first case (Figs. 1–3), which was run exclusively on a 96×16 mesh, the cases were done by running the design process first on a coarse 48×8 mesh for several (typically 10) cycles before moving on to the finer 96×16 mesh. On each mesh an airfoil shape that is compatible with the direct problem on that same mesh is generated. For most cases, after 10 design cycles on the first mesh, the maximum value of $|v/u|$ is reduced to less than 0.01. At this point the

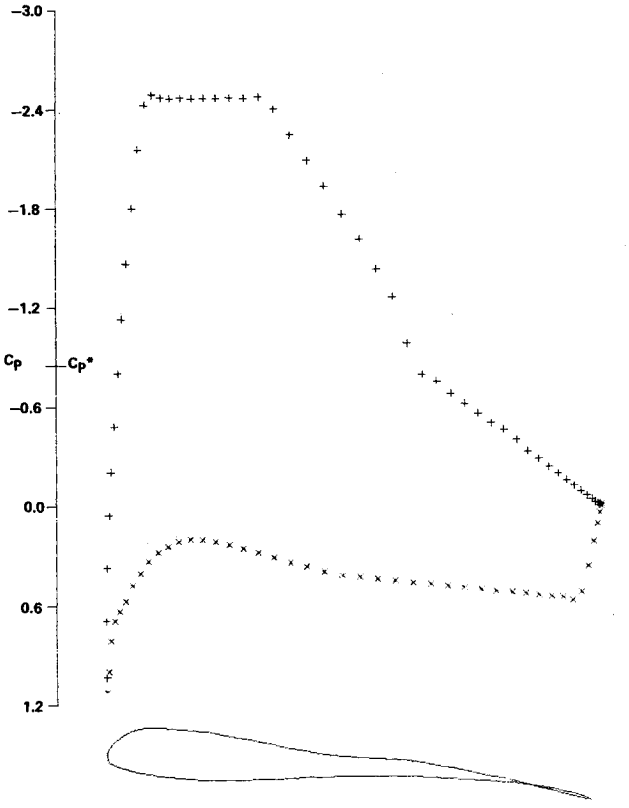

Fig. 11 Design case 645: contour and direct solution [$M_\infty = 0.683$, $C_L = 1.8071$ ($q_\infty = 0.994$)].

airfoil profile is usually within 1% of the final shape that would be obtained on that mesh. Convergence on a finer mesh using the shape designed on a coarser grid is, of course, much faster. The cases shown in this paper are intended as illustrations of the approach and, therefore, the tolerance levels to which the inverse design was taken were much smaller than necessary for engineering purposes. The cases shown in Figs. 9 and 10, which are examples of a much larger series of exercises, typically required about 30 min of computing time on an IBM 370/3033 computer, with about 15 design cycles on a coarse mesh and 10 on a fine mesh. In each of these design cycles, the tolerance levels on the maximum corrections are set to a value of 10^{-5} or smaller. Much faster strategies can be devised, however. In the early design cycles, there is no need to converge to these small tolerances. Only in the later cycles, as the final contour is approached, need the tolerances be set to very small values. Circle plane relaxation methods have a notoriously slow convergence rate in the radial direction. The relaxation solution in the Dirichlet inverse mode must be converged to a maximum correction level of 10^{-6} to compute a normal velocity component to four decimal places (further convergence would not change the value of this variable to within the four decimal places). In the direct problem, convergence to 10^{-5} is usually sufficient to obtain the same degree of accuracy on a computation of the tangential velocity component.

Some of the above cases have been rerun with different convergence strategies, resulting in a time saving as large as 70%. It should also be remembered that, in the last several years, there have been developed solution procedures such as approximate factorization and multigrid schemes that are faster than the relaxation method used here. Use of these schemes would reduce the required computational time by about one order of magnitude.

Conclusions

The purpose of this paper has been to point out the existence of closure conditions for the inverse problem of airfoil theory in transonic flow similar to conditions arising in incompressible flow. Failure of previous methods for transonic airfoil design to recognize the existence of the first closure condition in transonic flow has led to ill-posed formulations. The present analysis indicates that it is not possible to specify both the freestream speed and the speed distribution on the airfoil. As shown in the present approach, the prescribed speed distribution must satisfy a constraint if the freestream speed is prescribed, just as in the incompressible problem. The method is general, as seen by the number of examples presented. The desired pressure distribution can be arbitrary, if it contains an adjustable parameter or if the freestream speed is determined as part of the solution (both procedures are entirely equivalent).

The method can be extended to include trailing-edge closure conditions in a straightforward manner. Unlike the first closure condition, the trailing-edge gap can be monitored during a design procedure and changes in the target velocity distribution can be made to drive the gap to any desired value, just as in incompressible flow. It should be emphasized that the particular procedure for introducing the free parameter (the multiplication factor A) in the present method is only one of the many ways it can be introduced into the formulation to close the design problem. The present procedure can be modified so that changes applied to the target speed distribution needed to satisfy our solubility condition and to control trailing-edge closure are made only over selected segments of the airfoil profile in order that desirable features of the prescribed flow might be retained exactly. Schemes such as those developed by Arlinger,[4] Strand,[5] and Polito,[6] which minimize the changes, could be implemented in the present transonic flow method.

Acknowledgment

This investigation was partially supported by the Office of Naval Research through Contract N00014-78-C-0476.

References

[1] Lighthill, M.J., "A New Method of Two-Dimensional Aerodynamic Design," Aeronautical Research Council, London, R&M 2112, April 1945.

[2] Woods, L.C., "The Design of Two-Dimensional Aerofoils with Mixed Boundary Conditions," *Quarterly of Applied Mathematics*, Vol. 13, 1955, pp. 139-146.

[3] Van Ingen, J.L., "A Program for Airfoil Section Design Utilizing Computer Graphics," Agard Short Course Notes, April 1969.

[4] Arlinger, B., "An Exact Method of Two-Dimensional Airfoil Design," Saab, Sweden, Rept. TN67, Oct. 1970.

[5] Strand, T., "Exact Method of Designing Airfoils With Given Velocity Distribution in Incompressible Flow," *Journal of Aircraft*, Vol. 10, Nov. 1973, pp. 651-659.

[6] Polito, L., "Un Metodo Esatto per il Progetto di Profili Alari in Corrente Incompressibile Aventi un Prestabilito Andamento della Velocita' sul Contorno," Universita' degli Studi di Pisa, Pisa, Italy, Rept. 42, 1974.

[7] Woods, L.C., Aerofoil Design in Two-Dimensional Subsonic Compressible Flow," Aeronautical Research Council, London, R & M 2845, March 1952.

[8] Tranen, T.L., "A Rapid Computer Aided Transonic Airfoil Design Method," AIAA Paper 74-501, 1974.

[9] Carlson, L.A., "Transonic Airfoil Analysis and Design Using Cartesian Coordinates," *Journal of Aircraft*, Vol. 13, May 1976, pp. 356-369.

[10] Henne, P.A., "An Inverse Transonic Wing Design Method," AIAA Paper 80-30, 1980.

[11] Hicks, R.M., Vanderplaats, G.N., Murman, E.M., and King, R.R., "Airfoil Section Drag Reduction at Transonic Speeds by Numerical Optimization," NASA TMX-73097, Feb. 1976.

[12] Davis, W.M., "Technique for Developing Design Tools from the Analysis Methods of Computational Aerodynamics," AIAA Paper 79-1529, 1979.

[13] McFadden, G.N., "An Artificial Viscosity Method for the Design of Supercritical Airfoils," Courant Institute of Mathematical Science, New York University, New York, Research and Development Rept. C00-30770158, July 1979.

[14] Jameson, A., "Numerical Computation of Transonic Flows with Shock Waves," Paper presented at Symposium Transonicum II, Göttingen, FRG, Sept. 1975.

[15] Ludford, G.S., "The Behavior at Infinity of the Potential Function of a Two-Dimensional Subsonic Compressible Flow," *Journal of Mathematical Physics*, Vol. 30, 1951, pp. 117-130.